POLITECNICO
MILANO 1863

SCUOLA DI INGEGNERIA INDUSTRIALE
E DELL'INFORMAZIONE

EXECUTIVE SUMMARY OF THE THESIS

Dissecting Cabozantinib mechanisms of action and therapeutic efficacy in preclinical models of prostate and renal cancer lesions in bone

TESI MAGISTRALE IN BIOMEDICAL ENGINEERING – INGEGNERIA BIOMEDICA

AUTHOR: SILVIA BUSA'

ADVISOR: PIETRO CERVERI

ACADEMIC YEAR: 2023-2024

1. Introduction

Prostate cancer ranks as second cancer diagnosed in male globally and is a leading cause of cancer-related deaths, especially in Western countries. Renal cell carcinoma (RCC) is the most common type of kidney cancer, with its prevalence expected to increase worldwide. Both prostate and renal tumors have a high propensity to metastasize to the bones, leading to severe complications and reduced survival rates. Treatment decisions depend on several factors including the extent of bone disease, presence of other metastases, cancer type, prior treatments, symptoms, and overall health. While treatments can alleviate symptoms, they are not curative. Treatments for advanced prostate cancer like external beam radiotherapy and radiopharmaceuticals such as radium-223 are commonly used for impeding tumor growth. However, they may cause hematological toxicity or disease progression. Other treatment options include hormonal therapy, Abiraterone, immunotherapy, or combination therapies, but metastatic prostate cancer remains incurable. For metastatic RCC, interventions include anti-angiogenic tyrosine kinase inhibitors and immunotherapies, but the complete remission is rare, and advanced renal cell carcinoma remains a deadly disease. Among VEGF receptor tyrosine kinase inhibitors, cabozantinib represents a cost-effective option that it has been approved for the metastatic renal cell carcinoma treatment and is being considered for prostate cancer.

The objectives of this study are to investigate the effects of cabozantinib on blood vessels within bone metastases from prostate tumor and to evaluate whether effects of cabozantinib in RCC and prostate cancer are comparable. Indeed, despite being approved for RCC treatment, cabozantinib effects on bone lesions are obscure, mostly due to the absence of relevant models of bone metastasis. Moreover, a comparison on the impact of cabozantinib in blood vessels of prostate vs renal bone metastasis was never performed. In this study, a newly developed bone metastasis preclinical model was applied, using human-derived prostatic tumor cells (PC3) engrafted into nude mice tibiae, followed by oral administration of cabozantinib. Tumor-bearing bones were

recovered and underwent immunofluorescence staining. and multiphoton microscopy (MPM) acquisition. Image analysis was then performed that allowed blood vessels parameters assessment within the tumor area, including the percentage of area occupied by blood vessels, their shape and size, the distance between proximal blood vessels, and the proximity of a mitotic cell to the nearest blood vessel. The findings from this study are crucial in understanding the drug's potential effects on the vascular structures within bone metastases and may provide valuable insights into its efficacy across different cancer types. Furthermore, this study underscored the challenge of manually identifying mitotic and apoptotic cells in biological images and prompted the development of a new artificial intelligence-based system for the automatic recognition and quantification of mitotic and apoptotic nuclei, in collaboration with the Department of Electronics, Information and Bioengineering.

2. Materials and Methods.

Mice bearing prostate cancer bone lesions were orally administered cabozantinib, bone were then isolated and analyzed by immunofluorescence analysis. The focus was on studying the impact of this agent on the vascular structure of bone metastasis.

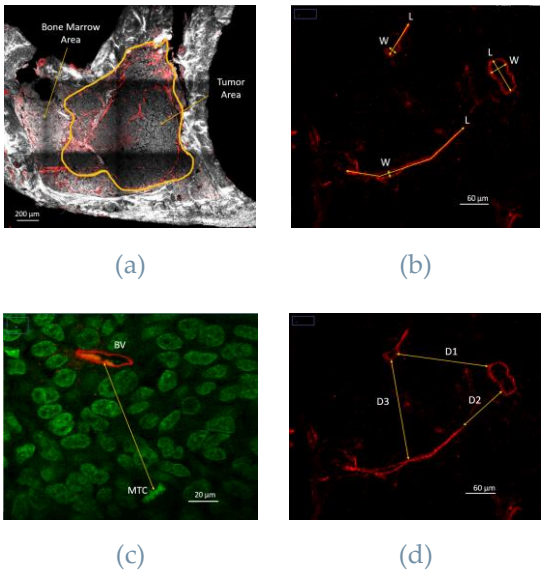

Figure 1: Evaluation parameters for metastatic bone microenvironment. (a) %BV inside tumor area: here a tibiae cross section with PC3 cells as tumor cells. PC3 are usually bigger than normal bone marrow cells. (b) BVs size; (c) MTC-BV distance; (d) BV-BV distances.

The images for the in vivo experiment were captured using MPM (Multiphoton Microscopy). Different parameters were quantified, see Figure 1, including the percentage of blood vessel area within the tumor region (a), vessels dimension (b), inter-vessel distance (d), and the proximity of mitotic cells to vessels (c).

To validate our findings, we analyzed bone lesions from renal tumors; data for this analysis were previously collected by the laboratory team. Cord blood (CB)-derived NK cells have been applied in leukemia patients with remarkable results (complete response in 7/11 patients) [141] and are currently being explored in a series of clinical trials, both in liquid and solid tumors [145]. An EVOS system was utilized to acquire images for in vitro experiments. Analyses were performed using Fiji software, an open-source image processing tool based on ImageJ2. This software enabled the visualization and the quantification of images/video obtained from both the EVOS system and MPM acquisition.

2.1. EVOS system

The EVOS imaging system includes a multichannel fluorescence or brightfield microscope and a supporting software. EVOS allows time-lapse movie acquisition, multi-well plate scanning, image stitching and tiling and cell counting, providing high quality images in no time, over time, every time. The EVOS system in this work was widely used to characterize PC3 cell line. It was extensively used to capture images and videos during various experiments.

2.2. Multiphoton Microscopy

Two-photon excitation microscopy, also known as multiphoton laser scanning microscopy (MPM), offers a superior approach to confocal microscopy, especially for imaging living cells within intact tissues. Confocal microscopy, while enabling three-dimensional sectioning in thicker tissues, suffers from issues like out-of-focus flare, photobleaching, and phototoxicity due to excitation light. In contrast, two-photon excitation provides precise three-dimensional optical sectioning without causing photobleaching or phototoxicity above and below the focus plane. This is achieved through the interaction of two photons with a single fluorophore at the laser's

focal point, allowing for deeper specimen penetration with reduced photodamage. Although multiphoton microscopy requires expensive laser equipment and a costly maintenance, its benefits for imaging thicker specimens make it a valuable tool, especially for research involving ex vivo animal samples, as utilized in this study at the MD Anderson Cancer Center genitourinary laboratory.

3. Results

3.1. In Vivo Studies

In order to study the impact of cabozantinib on blood vessels within bone metastases from prostate and renal tumors, in vivo studies were performed. Samples of bone metastatic renal cells were previously generated in the lab. Instead, to obtain data regarding prostate cancer bone metastases, new experiments were performed. Since human prostate cancer cells (PC3) were used, nude mice were applied. This mouse strain lacks mature T cells making them suitable for engrafting human cancer cells. PC3 cells were injected directly into both tibiae of the mice and after 3 days, treated mice received cabozantinib orally. Control and treated mice were euthanized after 7 or 10 days.

Tumor-bearing bones were collected, fixed in 4% PFA for 24 hours and decalcified in 0.5 M EDTA for 5 days. Bone samples embedded in agarose 4% were sliced to a thickness of 100 μm for staining and imaging was performed using MPM.

Immunofluorescence (IF) analysis was utilized to visualize specific components of the bone samples, including cell nuclei and tumor blood vessels. The indirect IF technique, employing primary and secondary antibodies, was chosen for staining blood vessels due to its sensitivity and signal amplification capabilities. Various antibodies were tested to enhance the fluorescence signal, with rat anti-endomucin combined with anti-rat AlexaFluor 680 ultimately providing the best results. DAPI staining was used to detect nuclei of bone marrow cells, while nuclei of PC3 cells also expressed GFP protein linked to the histone H2B.

Decalcified bone samples were initially sliced parallel to the bone's longitudinal axis for a wider field of view. However, visualizing tumor blood vessels proved to be challenging due to their complex arrangement. Transversal slicing was then performed to better visualize the blood vessels within the tumor area.

MPM allowed for the acquisition of three-dimensional samples through optical sectioning, with data collected in sequential stacks of images. Besides fluorescence emission, MPM captured nonlinear functions of light, including second harmonic generation (SHG) from collagen in bone. Overall, the acquisition process allowed nucleus, blood vessel, and bone visualization.

Images from the prostate model acquired through MPM were subjected to analysis. Initially, the percentage of blood vessel area within the tumor was quantified semi-automatically using ImageJ. Significant differences were observed between the control and treatment groups, aligning with cabozantinib's mechanism of action that consists of blocking angiogenesis, see Figure 2.

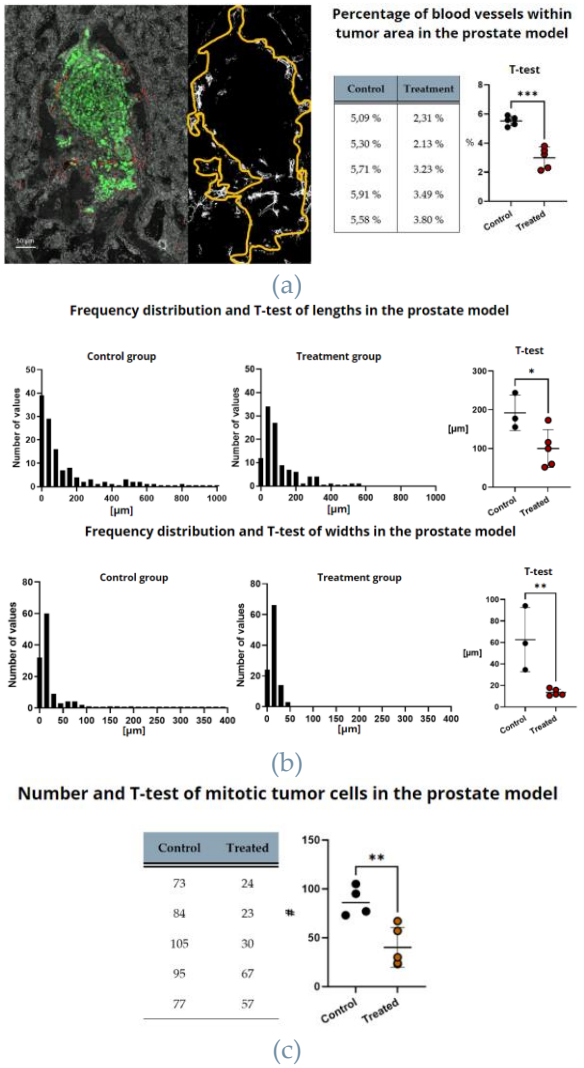

Figure 2. Results from the analysis of the prostate model: (a) %BVs within the tumor area; (b) dimensions; (c) mitotic tumor cell-blood vessel distance.

Further analysis compared blood vessel dimensions between treated and control samples, including length and width. While attempts were made to automate this process using ImageJ's Skeleton plugin, the complexity of the blood vessel network hindered automation, leading to manual tracing. Significant reductions in both length and width were observed (40% and 88%, respectively) in the treated group, particularly affecting larger vessels, see Figure 2.

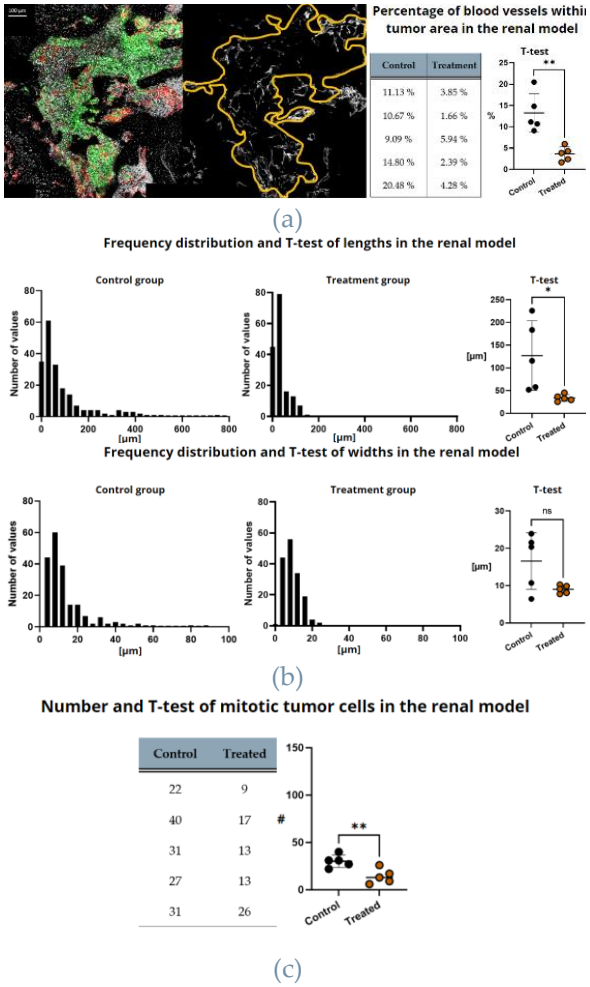

Figure 3. Results from the analysis of the renal model: (a) %BVs within the tumor area; (b) dimensions; (c) mitotic tumor cell-blood vessel distance.

The distance between adjacent blood vessels and the distance between mitotic cells and the nearest blood vessel were also analyzed. The former showed non-significant results, indicating no change induced by cabozantinib treatment; the latter remained unaffected, suggesting that mitotic cells nutrient requirements were independent of cabozantinib treatment. However, there was a notable decrease (47%) in the number of cells undergoing mitosis in the treated group, attributed to reduced blood supply due to cabozantinib's action, see Figure 2.

During analysis, apoptosis was observed, even though less frequently than mitosis. Manual discrimination of mitotic and apoptotic cells was time-consuming and required expertise, highlighting the need for automated tools. To address this, a new research project aiming at developing artificial intelligence for cell recognition was initiated,a s described below..

To validate the findings observed in another tumor type, a renal tumor model was examined. RENCA bone lesion images before and after cabozantinib treatment were already acquired by the laboratory's team. The analysis protocol followed the prostate model, yielding comparable results. Cabozantinib treatment led to a significant decrease (9%) in the percentage of blood vessels within the tumor area, although with less statistical significance compared to the prostate model. This variance could be attributed to the unique behavior of PC3 cells, which tend to form tumor clusters with minimal internal blood vessel presence, affecting the blood vessels percentages in the area. Comparisons of blood vessel-related parameters between treated and control samples revealed significant impacts on vessel dimensions, particularly affecting larger vessels. Notably, differences in blood vessel networks between the two metastatic environments were observed, with prostatic model vessels being fewer but longer and wider, while renal model vessels were more numerous but shorter and narrower. The distance between mitotic cells and proximal blood vessels did not show significant changes post-treatment, although there was a decrease in the number of mitotic cells. Interestingly, the maximum distance of a cell in mitosis from a blood vessel was shorter in the renal model compared to the prostate model. Overall, cabozantinib had a similar impact on bone lesions from prostate cancer as observed in the renal model, decreasing blood vessel numbers and sizes, thereby hindering tumor growth by depriving cells of essential blood supply for replication. However, the distance from a blood vessel remained consistent after treatment.

3.2. In Vitro Studies

As described above, we investigated the relationship between mitotic tumor cells and blood vessels. Due to the lack of automated tools for this task, the discrimination of mitosis or apoptosis was done manually, which was time-consuming and required expertise. To overcome this issue, we initiated a project to develop an artificial intelligence-based system for automatic recognition of mitotic and apoptotic nuclei. We employed a deep learning algorithm, with a U-Net neural network applied, trained with ground truth images, to automatically identify and segment biological structures. As part of my thesis work, I generated biological images and segmented nuclei to train the U-Net.
Several experiments were conducted to visualize cell division and apoptosis mechanisms thoroughly and to acquire expertise in discriminating them. Time-lapse recordings up to 24 hours were created to observe mitotic division stages, see Figure , and apoptosis development. Due to the limited presence of apoptotic cells observed in cell culture an experiment was conducted to induce apoptosis using three chemotherapy drugs: cisplatin, docetaxel, and doxorubicin. Images from the cisplatin and docetaxel experiments were utilized to create apoptosis discrimination masks for the computational model.

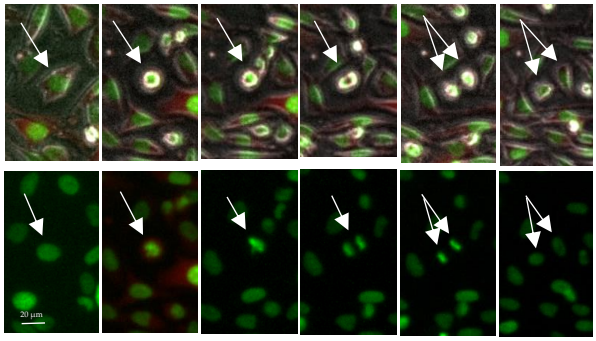

(a) (b) (c) (d) (e) (f)

Figure 4. interphase (a), prophase (b), metaphase (c), anaphase (d), telophase (e), and two distinct cells (f).

Specifically, see Figure 5, masks of mitotic and apoptotic cells from RGB images captured with the EVOS system were generated. Image segmentation was performed on 512x512-pixel patches containing mitosis and/or apoptosis events. These patches were duplicated and saved in their original format. From each duplicated patch, an 8-bit mask was generated using ImageJ, then converted into a 16-bit image. Stardist, an ImageJ plugin, was utilized to segment and label all nuclei with different colors. Due to irregular shapes of apoptotic cells, manual delineation of nuclei profiles was often necessary. Nuclei were color-coded: interphase nuclei in blue, nuclei in mitosis phases in yellow, and apoptotic nuclei in pink. Abnormal nuclei were not segmented. Both the mask and the original patch were used as inputs for the model.

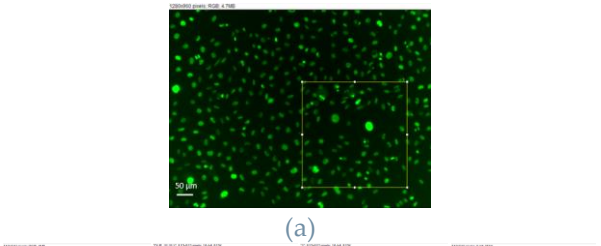

(a)

(b) (c) (d) (e)

Figure 5. Development of an 8-bit mask starting from RGB images acquired via the EVOS system. Selection of the frame(a); extrapolation of the patch (b); conversion in 16-bit (c); output from Stardist (d); (e)mask.

4. Discussion

This study investigated the effects of cabozantinib on bone lesions originating from prostate cancer, with subsequent validation using a renal model. Despite cabozantinib is being approved for RCC treatment, its effects on bone lesions are obscure, mostly due to the absence of relevant models of bone metastasis. A newly developed preclinical model using nude mice implanted with human derived PC3 cells was employed, followed by cabozantinib administration. Sample processing involved transverse slicing to enhance visualization of tumor blood vessels, stained using immunofluorescence, and imaged with MPM. Analysis via ImageJ revealed significant findings, including a reduction in blood vessel number and size within the tumor area, indicative of cabozantinib's action on VEGF receptors. Notably, vascular structure varied between tumor types, the prostatic model exhibited a less dense network

compared to the renal model. Blood vessels also showed different features, with longer and wider vessels compared to the renal tumors, which displayed shorter and narrower vessels, consistent with a highly angiogenic tumor type.
Cabozantinib had a greater impact on vessel number and length in the renal model (decreased by 9% and by 75%, respectively), while it had a more pronounced effect on vessel width reduction in the prostate model (decreased by 88%). Interestingly, cabozantinib did not affect the distance of mitotic tumor cells from the nearest blood vessels but indirectly decreased the mitosis number by diminishing the tumor's blood supply, leading to impaired tumor growth. Apoptotic cells were rare, suggesting that cabozantinib did not directly killed influence on tumor cells.
Recognizing mitotic and apoptotic cells required significant expertise and time, prompting the development of an artificial intelligence-based system for automatic recognition and quantification of these nuclei. The U-Net neural network system was trained with ground truth images to achieve automatic identification and segmentation of biological structures. Segmenting apoptosis was more complex than mitosis due to fragmented structures, necessitating manual intervention. Despite challenges, this process aims to automate future analyses, facilitating efficient and accurate cells discrimination for assessment of tumor dynamics and treatment responses.

5. Conclusions

Results showed similar impact of cabozantinib in both renal and prostate models, notably reducing the number and size of blood vessels within the tumor area. Additionally, it decreased tumor cell mitosis due to reduced blood supply, hindering tumor growth. These findings are noteworthy as cabozantinib demonstrated analogous effects in bone lesions from two different tumors, indicating its efficacy independent from the tumor cell type involved (whether renal or prostatic). Future studies may use different tumor cell lines for validation. Moreover, the data resulting from the analysis of the prostate model will serve as the basis for a computational model that will represent the development of bone metastases from prostate cancer, and the effects due to cabozantinib treatment. To automate mitotic and apoptotic cell recognition, a new project utilizing artificial intelligence was initiated, although further image quantification is needed for improved network performance.

References

[1] P. Maroto, C. Porta, J. Capdevila, A. B. Apolo, S. Viteri, C. Rodriguez-Antona, L. Martin and D. Castellano, "Cabozantinib for the treatment of solid tumors: a systematic review," *Therapeutic Advances Med. Oncol.*, vol. 14, p. 175883592211071, gen. 2022.

[2] J. Ban, V. Fock, D. Aryee and H. Kovar, "Mechanisms, Diagnosis and Treatment of Bone Metastases," *Cells*, vol. 10, no. 2944, 2021.

[3] D. W. Piston, T. J. Fellers and M. W. Davidson, "MicroscopyU," 2023 Nikon Instruments Inc., [Online]. Available: https://www.microscopyu.com/techniques/multi-photon/multiphoton-microscopy. [Accessed 31 12 2023].

[4] M. Sekhoacha, K. Riet, P. Motloung, L. Gumenku, A. Adegoke and S. Mashele, "Prostate Cancer Review: Genetics, Diagnosis, Treatment Options, and Alternative Approaches.," *Molecules*, vol. 27, no. 17, p. 5730, 5 sept 2022.

6. Acknowledgements

I would like to express my deepest gratitude to Dr. Dondossola for her support, for the knowledge transmitted and for practical suggestions during my research and in drafting the essay.
I'm extremely grateful to my advisor prof. Cerveri for his availability and promptness to all my requests.
I am also thankful to my family for their infinite love and constant support that allowed me to complete my university studies.
Finally, I would like to dedicate this achievement to myself, wishing it as the beginning of a long and brilliant professional career.